2018 7th IEEE International Conference on Biomedical
Robotics and Biomechatronics (Biorob)
Enschede, The Netherlands, August 26-29, 2018

Preliminary Design and Evaluation of a Single-Actuator Anthropomorphic Prosthetic Hand with Multiple Distinct Grasp Types

Michael T. Leddy, *Student Member, IEEE,* and Aaron M. Dollar, *Senior Member, IEEE*

Abstract— **The various drawbacks of complex myoelectric prosthetic hands have led to low adoption rates by upper limb amputees, with upwards of 35% pediatric device rejection and 23% adult device rejection rates. This paper describes the design of a novel 50th percentile female sized single-actuator anthropomorphic myoelectric hand that was created to address issues commonly associated with myoelectric prosthesis. The hand uses underactuated coupling mechanisms to enable three distinct passively-adaptive grasp types, from a single DC motor and single input control, selected through a simple manual reconfiguration of the digits. The hand was evaluated in a preliminary assessment that included benchtop evaluation and a five subject able-bodied combined Box and Blocks and SHAP test using a bypass socket to evaluate effectiveness on activities of daily living. The able-bodied subject testing results are presented and compared to published SHAP results from commercial powered hook, single-actuator anthropomorphic and multi-actuator anthropomorphic devices.**

I. Introduction

The last decade has seen significant advancements in upper limb prosthetics, especially in commercially-available multi-articulated hands. Many anthropomorphic commercial devices have a single actuator for each finger, allowing for the ability to form multiple grasp types. However, varying drawbacks of these devices have led to low adoption rates by upper limb amputees including up to 35% pediatric device rejection and 23% adult rejection [1]. This has been partly attributed to lengthened training and follow-up times, high power consumption, multiple electrode reliability, grasp adaptability, speed and motion of fingers, durability, weight, and cost. A robotic prosthetic hand that can replicate the human hand's 20 active degrees of freedom, 17,000 tactile sensors, up to 300°/s finger joint angular velocity [2] and exert above 25N of force at the distal finger with high medial-lateral force production [3], is far from feasible with current portable actuator and sensor technology.

These practical limitations have led to many designs that aim to approach the versatility of the human hand through the implementation of underactuated mechanisms [4][5], which can reduce the demanding control of fully actuated devices and passively adapt to objects being grasped. The differential coupling mechanisms in these hands transfer the actuation torque to larger contact areas, providing secure grasps with delicate handling [6]. These underactuated devices rely on differential mechanisms to couple the joints and/or fingers, such as transmissions [7], Geneva mechanisms [8], moveable pulleys, various geared differentials, and whiffletree mechanisms [9]. A significant number of these hands use two to three dc motors, typically actuating the forefinger and thumb flexion as well as the thumb position [10-12]. One design [13] grasps with a single actuator and uses an additional actuator to provide discrete starting postures. However, more than one actuator creates a tradeoff between maintaining anthropomorphism and actuator size. An underactuated hand with a single larger actuator provides power density and packaging benefits over several smaller actuators. Some single-actuator underactuated hands [14-16] have successfully used a single actuation input to control and balance forces in all five fingers with manually posable thumbs, while others have used mechanical means of fixating or varying finger motion [17]. Alongside force balancing and grasp adaptability, these hands are anthropomorphic, easy to control, durable, lightweight and low cost. However, single-actuator hands still lack the combination of distinct grasp types with varying force production, closing rates and excursion seen in more complex anthropomorphic hands [18][19].

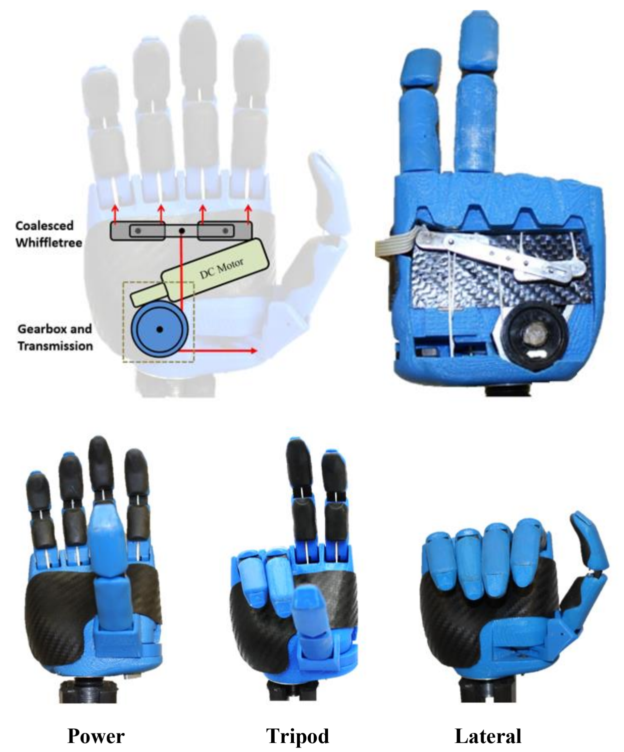

Figure 1. The Yale MyoAdapt Hand with three distinct grasp types, a five-fingered power grasp, three-fingered tripod grasp and lateral grasp. The transmission transfers torque to the whiffletree mechanism, which distributes force across the forefingers, and to the thumb through Spectra tendons. (Right) The whiffletree orientation and driving tendon positions in tripod grasp.

This work was supported by the US Army Medical Research and Material Command, under contract W81XWH-15-C-0125.All of the authors are with the Department of Mechanical Engineering and Materials Science, Yale University, New Haven CT 06511, USA, michael.leddy@yale.edu and aaron.dollar@yale.edu.

We propose a single-actuator anthropomorphic robotic prosthetic hand in which the thumb and finger positions are coupled together with multiple distinct grasp types (Fig. 1). This hand uses a combination of differential and other transmission mechanisms to allow the user to switch between three commonly used grasp types: power, tripod and lateral grasp [20]. The aim of this paper is to present the preliminary design and evaluation of this device to determine its feasibility, grasp topology, and functionality. This evaluation includes both benchmarking and able-bodied human subjects testing, to evaluate the preliminary performance of the hand across a range of metrics. Benchtop testing is used to evaluate the maximum grasp force and closing rate of the hand in each grasp type. Human subjects testing consisted of five participants who completed the Box and Blocks [21] and SHAP [22] tests to evaluate the hands performance in repetitive tasks and activities of daily living. These results were then compared to published results from other commercially available single and multi-actuator robotic prosthetic hands to lend insight into the hands' relative functionality.

II. Methods

A. *Single-Actuator Hand Design*

The Yale MyoAdapt Hand is a 50th percentile female sized anthropomorphic hand with a single degree of actuation that drives five two-jointed fingers for ten total degrees of freedom. The single actuation input is a brushed DC motor (*5.3 Watt Faulhaber 1524SR*, 6.98 mNm stall torque) attached to pulley-driven Spectra tendons that actively flex all five fingers using PID control. The fingers are passively extended by torsional springs at the metacarpophalangeal joint (MCP) and elastic flexures at the proximal interphalangeal joint (PIP). Finger position is controlled by a position controller that uses information from a high count 2-channel magnetic encoder as well as a current sensor used to detect contact. An additional degree of freedom is provided by a passive switch-locking rotational joint that allows the thumb to abduct and adduct orthogonal to either the palm or lateral index finger.

The palm of the hand is anthropomorphically sized [23] including MCP joint locations which are accurate in relative elevation, lateral positioning and abduction angle. The palm of the prototype hand is a 3D-printed ABS plastic shell with features to mount the internal transmission mechanisms. The front of the palm has urethane gripping surfaces to help secure objects in a caged grasp and the bottom of the palm has a standard ½"-20 threaded post for socket integration. There is a void by the wrist to allow for rotational abduction and adduction of the thumb. This area also houses the spring-loaded button mechanism that allows for repositioning of the thumb MCP joint. This mechanism is located on the bottom of the palm and can be pressed using affordances to aid thumb rotation. This is particularly important for bilateral amputees who may have issues when complex sequences of motions are required to move the thumb position.

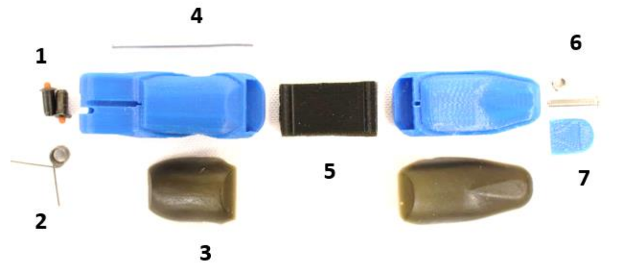

Figure 2. Modular underactuated finger components including (1) spring plunger pin joint (2) torsional spring (3) grip pads (4) low-friction tubing (5) flexure joint (6) tensioning mechanism (7) fingernail.

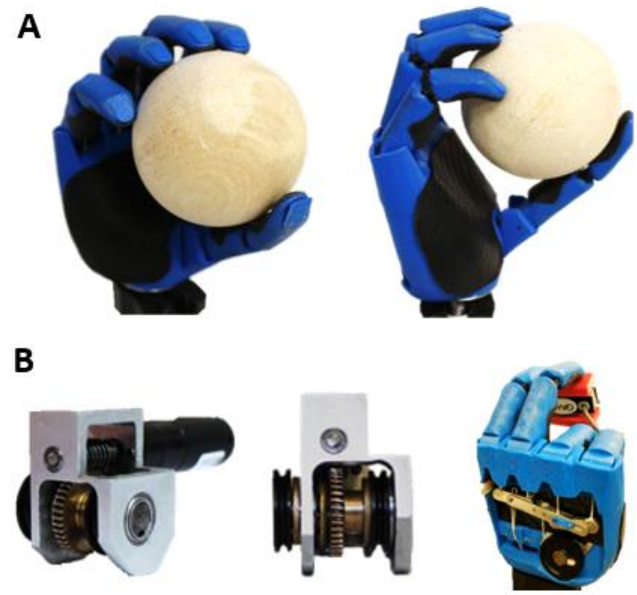

Figure 3. Examples of the underactuated grasping response. (A) Finger adaptability in power grasp around a spherical object from the SHAP test (B) Gearbox transmission that couples the single actuator to the forefinger and thumb driving tendons (left) and whiffletree reorientation in power grasp of a small object (right).

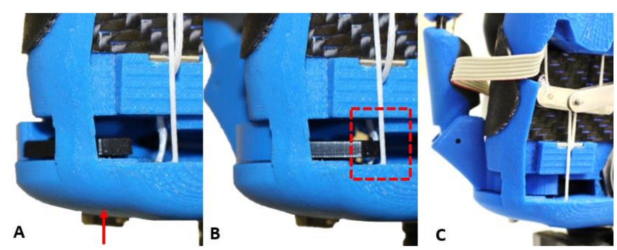

Figure 4. The sequence to switch between power / tripod grasp to lateral grasp includes (A) pushing the release button (B) rotating the thumb applying a force to an additional tendon on the index-middle pair (C) locking the thumb in lateral position, anchoring the fingers closed.

The fingers of the single-actuator hand are tendon-driven underactuated anthropomorphically-sized [23] fingers with two joints (Fig. 2). Each finger includes an MCP joint passively extended by a torsional spring, an elastic flexure PIP joint, a distal tensioning mechanism, grip pads and a fingernail. A spring plunger pin joint attaches the finger to the base at the MCP joint, allowing the finger to eject under lateral or other unfavorable loading conditions and can easily be reattached. The elastic flexure PIP joint allows for out-of-plane motion and passive reconfiguration of the distal link, promoting the adaptability required for a wrap grasp of a non-uniform object. This flexure has embedded cloth on the neutral axis to mitigate axial stretch, adding kinematic precision and creating a smooth bending motion during finger actuation. Finger flexure geometry, durometer and cloth location were investigated to determine optimal finger motion, input force to closing force, hysteresis and stiffness. A tensioning mechanism in the distal end of the finger consists of a cannulated screw that holds the terminated screw knots, and a hex nut that is integrated into the distal link. This is used to even the pretension in each finger to ensure uniform closing rates and force transmission. This mechanism is located under a fingernail which helps grasp small thin objects. Due to the rounded nature of the anthropomorphic fingers, the fingertips and distal fingernails have a flat surface to help prevent ejection of smaller objects during tripod and power grasp. There are several friction reduction mechanisms, such as flared tubing in the fingers and v-groove pins in the palm, that help reduce friction from tendon redirection.

The power is transferred from the actuator to the five fingers using a custom transmission and force balancing whiffletree mechanism displayed in Figs. 3 and 5. The transmission connects to the planetary stage of the actuator through a single-start worm gear pair. This non-backdrivable mechanism allows the hand to maintain grasp force for each motor position without requiring constant exertion from the motor. The worm gear is attached to a pulley transmission that couples the motor force to two driving tendons, one for the thumb and one for the forefingers seen in Fig. 3. The two coaxial pulleys rotate on a keyed shaft and have holes to anchor the driving tendons. The forefinger pulley is located outside of the gearbox in plane with another underactuated coupling mechanism while the thumb pulley is located inside the gearbox in plane with the thumb in lateral position. The pulley radius for each tendon is identical to ensure a similar closing rate and balance the opposing torques of the thumb and forefingers. All the fingers have a similar required excursion to fully close, meaning the pulley radius ratio could be adjusted to provide different closing rates and applied torques to better suit the user.

The forefinger driving tendon connects to a coalesced two member whiffletree. This mechanism allows tendon force to be even distributed among the forefingers, allows movement of the forefingers after single finger contact and provides an adaptive human-like grasping response. The connecting link in our whiffletree is coalesced allowing the finger bars to pivot within the driving bar. This reduces the mechanisms size and required travel, similar to the whiffletree layout in windshield wiper blades, however, it slightly limits the independent finger movement. The two outputs connect the index-middle and ring-pinky pairs where motion is inversely coupled. Our group has investigated using floating pulleys [24] to alleviate forefinger motion constraints. The second tendon from the transmission travels through the palm to the opposite side of the palm to drive the thumb.

The differential tendon routing that splits output from the motor to the eight joints of the forefingers and two joints of the thumb provides a high degree of underactuation that allows the hand to be controlled with single input control. The coalesced whiffletree allows for an adaptive underactuated grasp behavior that allows for increased conformation and contact locations with grasped objects. The routing of the tendon passively over the finger joints and the elastic PIP flexures each aid the underactuated grasp response within each finger, allowing out of plane motion and improved passive reconfiguration around objects (Fig. 3). The high degree of underactuation decreases the relative cognitive burden associated with controlling the device when compared to other devices with additional actuators and similar degrees of freedom.

The hand is capable of three distinct grasp types, a power grasp, a tripod grasp and a lateral grasp, that were chosen based on their frequency in everyday activities [20]. The combination of thumb movement and locking the ring-pinky member of the balance bar changes the grasp type of the hand, acting like a transmission that alters the forces, closing rates, timings and fingers used for each grasp type seen in Fig. 5. In power grasp, the thumb opposes the index and middle fingers and each finger closes at an identical rate until contact. The motor torque is equally distributed between the balanced forefingers and the thumb. The whiffletree allows additional finger reconfiguration and changes in grasp force to occur if one finger does not contact the object. In tripod grasp, the ring-pinky member of the whiffletree is locked down creating a new lever arm driving motion. The starting grasp position is altered to remove all driving tendon slack from the system, introduced from locking down one side of the whiffletree. The index-middle pair then closes on the thumb at twice the closing rate with the same force in power grasp. This is because although the new actuation lever arm is reducing the tendon force only two of the four members are receiving torque from the transmission. This provides a quick tripod grasp, however, reduces the potential grip force and creates a slight force imbalance between the thumb and opposing fingers. In lateral grasp, a spring-loaded button located on the bottom of the palm is pressed to rotate the thumb to lateral opposition. This button releases a spring plunger located on the bottom of the thumb block that holds the thumb in the power and lateral positions. The spring plunger then slides in a slot until the thumb reaches the next position where it automatically locks into place. The thumb rotation displaces a tendon, which is normally slack, connected to the index-middle whiffletree pair which also slightly closing the thumb seen in Fig. 4. This closes the remaining fingers of the hand and locks them into place. In lateral grasp, the forefingers are rigidly locked down by the thumb rotation, providing the user with a passive hook grasp that can be used to fixate or carry objects with no motor expenditure or an active lateral grasp that receives all the actuator torque. The grasp types are currently set manually, however, we have investigated methods to mechanically automate these changes [14] so that the full hand functionality and each grasp type can be

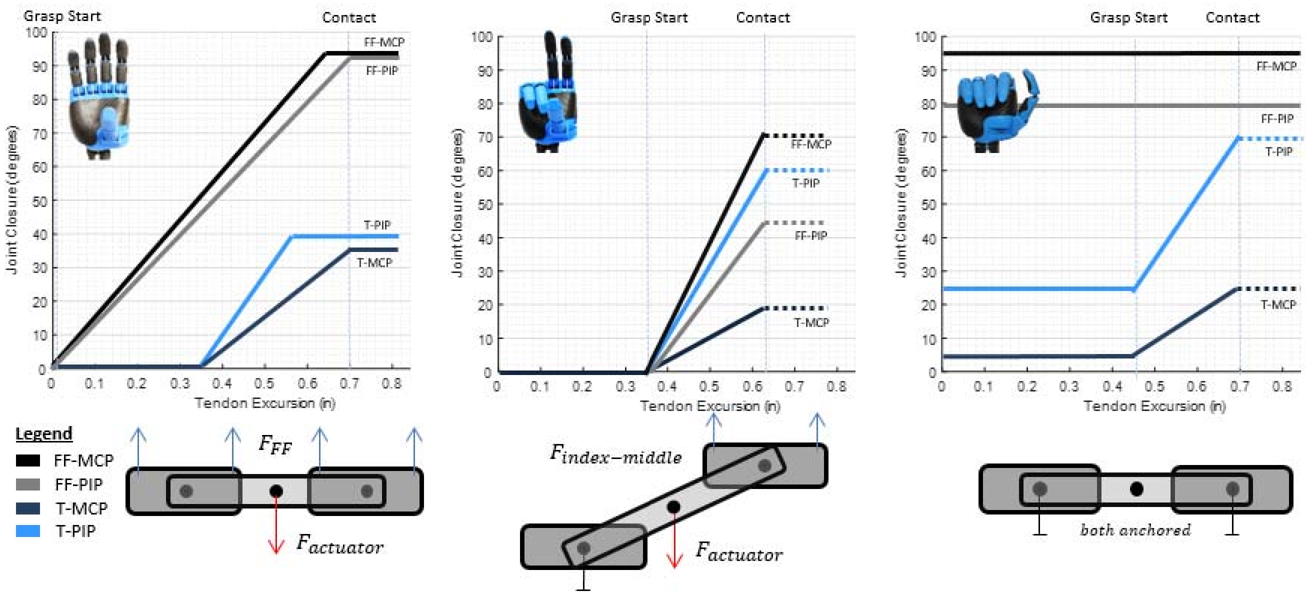

Figure 5. Grasp closing rates (displayed in depth in Tables 1 and 2) for the thumb (T) and forefinger (FF) joints along with the coalesced whiffletree orientation and hand posture for power, tripod and lateral grasps. The grasp starting and contact locations are noted for each grasp relative to total tendon excursion of the transmission. Dotted lines represent the potential for reorientation with additional force in the underactuated finger.

controlled from a single actuator with a single input. A successful grasp is determined by the motor controller when the actuator has either reached the final position for the given grasp type or a current limit is reached, notifying that an object has been grasped by the hand. The current limit while grasping is determined as a safe value for intermittent usage of the actuator; this value could be increased or decreased depending on the user's preference.

The Yale MyoAdapt Hand is fabricated using a variety of molding, machining and additive manufacturing techniques. The hand is also highly customizable including custom geometry grip pad molds created in a polyjet 3D printer and potential scalability of the palm and finger chassis to larger sizes. The hand materials include ABS plastic for the palm chassis, finger bodies and thumb block; urethane rubber for the grip pads (*Vytaflex 40*) and flexure joints (*PMC 780*), aluminum for the power transfer components, spring steel MCP torsional springs, and stainless steel for spring plungers, flared guiding tubing, bearings, screws and v-groove pins.

B. *Preliminary Evaluation*

In benchtop testing, two custom sensor embedded objects and a hand grasp force dynamometer (*Camry EH101 Digital Dynamometer*) were used to evaluate the maximum grasp force in each grasp type displayed in Fig. 6. Two average measurements were taken in power grasp using a 2.5in diameter sphere with an embedded load cell (*Transducer Techniques MLP-25*) and the 2in span grasp dynamometer. A 1.5 in span cube with an embedded load cell was used to evaluate the fingertip force in precision and lateral grasp. In each test the devices were fixated for distal link contact and the motor was run to stall at the continuous operating voltage within the current thermal limit. It is noted that distal contact produces less contact force than proximal contact in the underactuated fingers. Less contact force is observed at a constant actuation radius for smaller grasp spans that require more finger and passive elastic element motion.

The time to close the hand in each grasp was determined using the time difference measured in the motor controller software (*Faulhaber Motion Manager*) between when the command was signaled and when the encoder reached the final position. The final joint angles for the MCP and PIP joint for the forefingers and thumb were recorded at the end of each grasp using a goniometer and divided by the total closure time to receive the average finger angular velocity for each grasp type. It is noted that the closing rate of each finger varies with angular position and the closing rate of the anthropomorphic forefingers vary slightly due to the slight differences in link length. Starting aperture of each grasp was then measured as the distance between the distal thumb and distal link of the opposing members for each grasp.

The able-bodied testing consisted of five subjects, 4 males and 1 female, who are right hand dominant with no impairments (average age 24.6) and no previous usage of the device (HIC #1608018242). The testing consisted of five minutes of training where subjects could practice grasping sample objects. Next, each subject completed five trials of the Box and Blocks test, where the subject moves as many cubes as possible from one box to another within one minute to evaluate rapid grasping, holding and repetitive motion. Last, each subject completed a full Southampton Hand Assessment Procedure consisting of 26 tasks, 12 abstract object and 14 activities of daily living, recording the time to complete the task. In this test, subjects are encouraged to practice the task sufficiently and attempt to perform it as fast as possible. The Index of Function scores is then generated where an approximate score of 100 represents unimpaired human function, which varies by participant [25] but is nominally accepted. Testing was completed using an able-bodied adapter (*TRS Prosthetics*) to rigidly connect the prosthetic hand to the user. A mechanical button was used to simulate a single myoelectric input to open and close the hand. This was removed to focus on device performance as well as decrease the training time commonly associated with sEMG control. If required, grasps were switched manually in between tasks in the SHAP test.

C. Commercial Device Comparison

The preliminary Box and Blocks and SHAP performance of the Yale MyoAdapt Hand was compared to the performance of similar myoelectric terminal devices. In [26], eight trans-radial amputee subjects with significant myoelectric experience completed static wrist trials of the Box and Blocks and SHAP test using a single actuator hook (*Motion Control ETD ProPlus*) and a single actuator tripod gripper with an anthropomorphic glove (*Ottobock DMC plus*). In [27], six trans-radial amputees with significant myoelectric experience completed passive wrist trials of the Box and Blocks and SHAP using a two actuator myoelectric (*Ottobock Michelangelo)* anthropomorphic prosthetic hand. In [28], a single wrist disarticulation amputee with significant myoelectric experience evaluated two versions of a five finger anthropomorphic prosthetic hand with five actuators (*Touch Bionics i-Limb, i-Limb Pulse*) using the SHAP test with slight supination and pronation. Both studies included up to a month in training and practice with the device before completing the functionality assessment. It is noted that grasping techniques employed may differ between subjects with minimal wrist motion [28] and passive wrist motion seen in [26][27] and our study. In evaluation metrics, such as the Box and Blocks and SHAP tests, it is difficult to evaluate device performance without evaluating the user's ability and experience with the device.

III. Results and Discussion

A. Maximum Grasp Force Testing

The average maximum grasp force using sensor embedded objects was 15.21N in power grasp for a 2.75in diameter cylinder, 3.56N in tripod grasp of a 1.5in cube and 18.20N in lateral grasp of a 1.5in cube. In power grasp, the hand was able to grasp the dynamometer with 19.61N at a grasp span of 2in. The increase in dynamometer power grasp force from a smaller span could be due to loss of force from moments in the cylindrical testing setup. When compared to commercial multiple grasp type anthropomorphic hands with multiple actuators the force production is rather low in tripod and power but similar in lateral [29]. This could be due to off-axis force losses when using a single-axis load cell or extreme distal contact in tripod and precision, however, it is difficult to compare because the exact methods of evaluating force production vary by paper. Notwithstanding, the force production in the Yale MyoAdapt Hand was still significant enough to grasp and lift each object in the SHAP test. The tripod grasp produced significantly low force partly due to an inefficiency and force reduction that occurs in the whiffletree when one member is anchored. This lever arm produces twice the closing rate but halves the force which

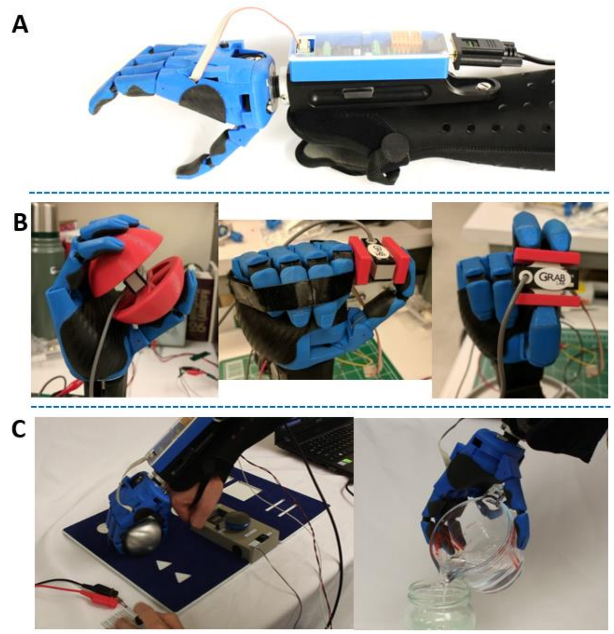

Figure 6. (A) Able-bodied test setup including prosthetic simulator with mounted prosthetic hand and control board (B) Sensor embedded objects used to measure force production in each grasp during benchmarking. (C) Able-bodied participants completing a SHAP task and general pouring task.

should be addressed in future versions. Last, operating at continuous operating voltage and current limits the hands potential grasp force. Due to the inherent intermittent motion of grasping, there are methods to increase grasp force by operating at currents and voltages above continuous operation for short durations. This is something we could investigate in the future, however, this leads to excessive heating and could potentially harm the electronic components.

B. Kinematic Analysis

The measured grasp aperture for the power and tripod grasp were 113.8 mm due to identical starting positions and the grasp aperture of lateral grasp was 25.4 mm opposing the lateral index finger. The joint range of motions in each grasp type, measured with a digital goniometer, was recorded in Table 2. The thumb motion was significantly less in power grasp because the thumb is delayed and is obstructed by the closing forefingers. In lateral grasp, the thumb rotation causes a slight excursion creating a smaller motion that starts with the thumb partially closed. In tripod grasp, the fingers contact one another before full joint closure in the forefingers and thumb. The average closing time in was 1.113 seconds in power grasp, 0.476 seconds in tripod grasp and 0.508 seconds in lateral grasp. Tripod grasp was quicker on average than power grasp because the required motion envelope is reduced and a lever arm caused by anchoring half of the whiffletree doubles the closing rate of the forefingers. The lateral grasp was rather slow for its aperture, however, is the strongest of the three grasp types. In [30], the recommended closing rate for a tripod grasp should not exceed 0.8 seconds with a span greater than 90mm to have minimal effect on proprioception. In [31], adequate full closure of the hand in any grasp should be from 1 to 1.5 seconds. Our tripod grasp falls within dictated specifications in [30], however, it may be advantageous to increase the speed of the power grasp which falls outside this recommendation but within those in [30]. When compared to the closing rates of the fully actuated anthropomorphic Bebionic V3 Hand [18], our hand has a slower power grasp (1.1 seconds compared to 0.5 seconds) but a faster tripod and lateral grasp (0.5 seconds compared to 1 second for both grasps). This shows promise for a single actuator hand on tasks that require precision or small motions. Power grasp speed can be addressed by adjusting the pulley ratios in the gearbox, however, this reduces the maximum tendon force output.

The Yale MyoAdapt Hand closing rates are displayed in Table 1. Our hand is not close to the 300°/s capability of the human hand, however is rather quick for its force production. In [2], it is rare to see human finger angular velocities exceed 100°/s during grasping, including approximately 50% human grasping with all finger angular velocities under 10°/s. The speed of the hand is promising, approaching joint angular velocities of near or above 100°/s for all three grasp types. There is a discrepancy into why the tripod grasp, only half the joint range of motion with faster finger closure, is not twice as fast as the power grasp which should be assumed by the grasp topology and whiffletree kinematics. This is because as the hand is closed the pulley radius about the MCP joint increases, decreasing the force required to produce a given torque. This mechanical force increase occurs at a quicker rate than the linear spring force increase, causing the fingers to accelerate across the trajectory until contact. The force increase also places the actuator at a more favorable point on its load curve making the stall torque at a given voltage higher. This also explains the rapid motion of the thumbs PIP joint which starts significantly pre-flexed during lateral grasp. The closing rates and joint angular velocities of the hand can be decreased to align more with [2][31] to align the grasp force with that of the fully actuated commercial prosthetic devices in [29].

C. Preliminary Hand Assessment

The Yale MyoAdapt Hand successfully transferred 19.1 blocks (σ = 3.84, low: 11 high: 27) on average over the course of a minute. On average there were 3.7 unsuccessful grasp attempts in each trial; occurrences when the subject closed the hand and was not able to grasp a block. For the SHAP test, the average IoF of the Yale MyoAdapt Hand was 82 which is promising for a robotic prosthetic hand with any grasp topology and actuator count. The full index of function distribution by participant is displayed in Fig. 7. Our hand struggled on the tip grasp, scoring a 50.2 on average across participants. This could be due to the weak precision grasp and slightly different closing rates between the index and middle fingers. Additionally, slight variations in tendon tension, either from inaccurate pre-tensioning or stretching, can cause grasp misalignment for all three grasp types. We expected using a button as the input source to marginally aid certain tasks, such as the Box and Blocks and the SHAP abstract object tasks, however, also increase the time to

TABLE I. BENCHMARKING RESULTS

Grasp Type	Grasp Specifications		Average Angular Closing Rates (°/s)			
	Grasp Force	*Closing Time*	*FF MCP*	*FF PIP*	*T MCP*	*T PIP*
Power	15.2 N	1.113 s	84.7	84.4	29.7	36.8
Tripod	3.6 N	0.476 s	145.0	99.8	39.9	136.5
Lateral	18.2 N	0.508 s	0 (fixed)	0 (fixed)	35.4	126.0

a. Only the index and middle finger are actuated in tripod grasp at twice the rate.

TABLE II. KINEMATIC CHARACTERISTICS

Grasp Type	Grasp Aperture	Range of Motion (°)			
		FF MCP	*FF PIP*	*T MCP*	*T PIP*
Power	113.8 mm	0-95	0-95	0-35	0-40
Tripod	113.8 mm	0-70	0-45	0-20	0-60
Lateral	25.4 mm	95-95	80-80	5-25	25-65

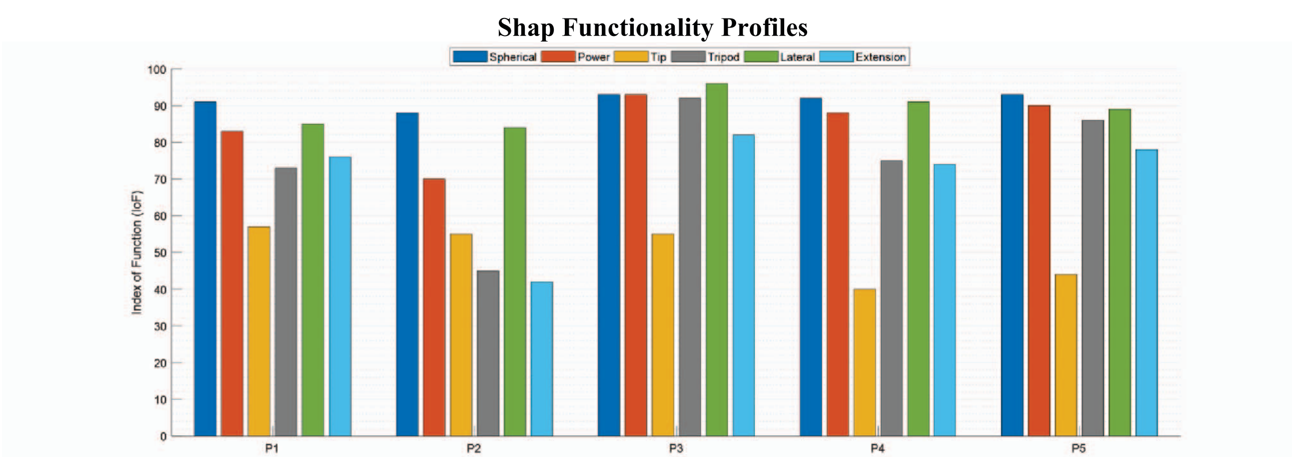

Figure 7. The SHAP functionality profile for each participant in the able-bodied trials. The single actuator hand and our participants scored highly in spherical (μ = 91.6), power (μ =84.8) and lateral ((μ = 89.0), had some difficulties in tripod (μ = 74.2) and extension (μ =70.4), and struggled in tip (μ = 50.2). The overall average index of function for all five participants was 82 where 100 represents able-body function.

complete bimanual tasks, such as the SHAP button board and jar lid. We believe this advantage would be mitigated when compared to someone with significant myoelectric training. The average Box and Blocks and SHAP index of function (IoF) scores are displayed in Table 3**.**

TABLE III. COMPARATIVE EVALUATION

Test	Prosthetic Device					
	Yale	*ETD*	*DMC*	*Michelangelo*	*i-Limb*	*i-Limb Pulse*
Box and Blocks	19.1	16	16	24.5	NA	NA
SHAP	82	58	51	82	52	88

D. Comparison to Commercial Devices

When compared to a single-actuator robotic split hook in [25] (*Motion Control ETD Proplus)* our hand performed 19.3% better on the Box and Blocks and 41.3% better on the SHAP test. When compared to a single-actuator anthropomorphic robotic tripod grasper [26] (*Ottobock Transcarpal DMC Plus)* our hand performed 19.3% better on the Box and Blocks and 60.8% better on the SHAP test. Although all the devices have a single actuation input, the relative increase in performance on the SHAP test, focused on activities of daily living, could have been bolstered by the ability to have more than one grasp type. This would provide less of a benefit on the SHAP test where a simple split hook and tripod grasper could suffice. In both evaluations the wrists were secured in their neutral positions. In [65] amputee subjects with significant training used myoelectric control while in our study a mechanical button was used for able bodied testing. We believe that novice users with a button would provide only a slight advantage, if any, over a trained prosthetic user.

When compared to a two actuator anthropomorphic robotic prosthetic hand [27] our hand performed 31.7% worse on the Box and Blocks and similar on the SHAP test after three months of practice. When compared to a fully actuated five actuator anthropomorphic robotic hand [28] (*Ossur Touch Bionics i-limb)* we performed 57.7% better on the SHAP test after one month of practice and 7.8% better after one year of practice with the i-Limb device. Compared to the newer device (*Ossur Touch Bionics i-Limb Pulse*), our hand performed 7.3% worse after one month of practice and 6.1% worse after four months of practice with the device. Our hand had similar results in the SHAP over the two actuator hand with a static wrist, however, our hand lacked in the Box and Blocks. This could be due to the Yale MyoAdapt Hand's weak precision grasp compared to the Michelangelo's two motor precision grasp and the significant training time allowed for the participant. Minimal grasp variety in the Michelangelo hand could have been a negative component to the overall index of function. Compared to the five actuator hands our hand performed favorably against the i-Limb and slightly worse than the i-Limb Pulse. Although there is only one participant in [28], he had the ability to actively flex and extend his wrist which could provide a benefit in the SHAP test for complex motions. All amputee subjects in [27][28] had significant training with myoelectric control which should have provided minimal benefit over the button.

IV. CONCLUSION

Overall, the Yale MyoAdapt Hand is a single-actuator anthropomorphic hand with novel finger design, underactuated coupling mechanisms and multiple distinct grasp types with different grasp force, closing rates and tendon excursions. This hand showed promise for single-actuator anthropomorphic robotic prosthetic hands with favorable performance in closing rate and varied grasp topography. This included favorable performance in the Box and Blocks and SHAP tests when compared to other single actuator terminal devices, the split hook and a tripod grasper, an anthropomorphic two actuator robotic hand and two fully actuated anthropomorphic commercial devices. Our hands grasp force will need to be improved to match the other commercial and simple graspers force. This can be accomplished by adjusting the pulley radius ratios in the transmission. The full hand has a mass of 290 grams without a battery and sized 50^{th} percentile female, making it significantly lighter and smaller than all the adult robotic prosthetic devices in [29]. The performance of the preliminary version of our hand when compared to other commercial terminal devices shows promise for single actuator anthropomorphic hands as a relatively effective replacement for the human hand.

REFERENCES

[1] E.A. Biddiss and T.T. Chau. "Upper limb prosthesis use and abandonment: A survey of the last 25 years." *Prosthetics and Orthotics International*, Vol. 31, No. 3, pp. 236-257, 2007.

[2] J.N. Ingram, K.P. Körding, I.S. Howard and D.M. Wolpert. "The statitstics of natural hand movements." *Experimental Brain Research*, Vol. 188, No. 2, pp. 223-236, 2008.

[3] F.J. Valero-Cuevas, F.E. Zajac and C.G. Burgar. "Large index-fingertip forces are produced by subject-independent patterns of muscle excitation." *Journal of Biomechanics*, Vol. 31, 1998.

[4] T. Laliberté and C.M. Gosselin. "Underactuation in robotic grasping hands." *Journal of Machine Intelligence and Control*, Vol. 4, No.3, pp.77-87, 2002.

[5] S. Hirose and Y. Umetani. "The development of soft gripper for the versatile robot hand." *Mechanism and Machine Theory*, Vol.13, pp.351-358, 1978.

[6] L. Birglen, T. Laliberté and C.M. Gosselin. *Underactuated Robotic Hands*. Springer-Verlag, ch. 2, 2008.

[7] M.C. Carrozza, C. Suppo, F. Sebastiani, B. Massa, F. Vecchi, R. Lazzarini, M.R. Cutkosky and P. Dario. "The SPRING Hand: Development of a Self-Adaptive Prosthesis for Restoring Natural Grasping," *Autonomous Robots*, Vol. 16, pp. 125-141, 2004.

[8] M. Controzzi, F. Clemente, D. Barone, A. Ghionzol and C. Cipriani. "The SSSA-MyHand: A Dexterous Lightweight Myoelectric Hand Prosthesis." *IEEE Trans. on Nueral Systems and Rehabilitation Engineering*, Vol.25, No. 5, pp. 459-468, 2017.

[9] L. Birglen and C.M. Gosselin. "Force Analysis of Connected Differential Mechanisms: Application to Grasping." *The International Journal of Robotics Research***,** Vol. 25, No. 10, 2006.

[10] J.L. Pons, E. Rocon, R. Ceres, D. Reynaerts, B. Saro, S. Levin and W. Van Moorleghem. "The MANUS-HAND Dexterous Robotics Upper Limb Prosthesis: Mechanical and Manipulation Aspects." *Autonomous Robots,* Vol.16 pp. 143-163, 2004.

[11] B. Peerdeman, M. Valori, D. Brouwer, E. Hekman, S. Misra and S. Stramigioli. "Uti Hand I: A lock-based underactuated hand prosthesis." *Mechanism and Machine Theory*, Vol.78, 2014.

[12] Ottobock Michelangelo Product Brochure, 2018. https://www.ottobockus.com/media/local-media/prosthetics/upper-limb/michelangelo/files/michelangelo-brochure.pdf.
[13] M.G. Catalano, G. Grioli, E. Farnioli, A. Serio, C. Piazza and A. Bicchi. "Adaptive synergies for the design and control of the Pisa/IIT SoftHand." *The Int. Journal of Robotics Research*, Vol.33, No. 5, pp. 768-782, 2014.
[14] J.T. Belter and A.M. Dollar. "Novel Differential Mechanism Enabling Two DOF from a Single Actuator: Application to a Prosthetic Hand." *IEEE Int. Conf. on Rehabilitation Robotics*, Washington, USA 2013.
[15] C.M. Gosselin, F. Pelletier and T. Laliberté. "An Anthropomorphic Underactuated Robotic Hand with 15 Dofs and a Single Actuator." *IEEE Int. Conf. on Robotics and Automation,* California, USA, 2008.
[16] K. Xu, H. Liu, Z. Liu, Y. Du and X. Zhu."A Single-Actuator Prosthetic Hand Using a Continuum Differential Mechanism." *IEEE Int. Conf. on Robotics and Automation*, Washington, USA, 2015.
[17] M. Baril, T. Laliberté, C. Gosselin and F. Routhier. On the design of a mechanically programmable underactuated anthropomorphic gripper. *ASME Journal of Mechanical Design*, Vol.135, No.12, 2013.
[18] Ottobock Bebionic V3 Product Brochure, 2018. http://bebionic.com/distributor/documents/bebionic_information_for_users.pdf.
[19] Ossur Touch Bionics i-Limb Quantum Product Brochure, 2018. http://www.touchbionics.com/sites/default/files/files/MA01336USrev20January2017/-limbquantum.pdf.
[20] I.M. Bullock, J.Z. Zhang, S. De La Rosa, C. Guertler and A.M. Dollar. "Grasp Frequency and Usage in Daily Household and Machine Shop Tasks." *IEEE Trans. on Haptics*, Vol. 6, No. 3, 2013.
[21] G. Volland, N. Kashman and K. Weber. "Adult Norms for the Box and Blocks Test of Manual Dexterity." *The American Journal of Occupational Therapy*, Vol. 39, No. 6, 1985.
[22] The SHAP Test Protocol and Procedure. www.shap.ecs.soton.ac.uk.
[23] A.R. Tilley. *The Measure of Man and Woman: Human Factors in Design.* John Wiley and Sons, New York, 2002.
[24] J.T. Belter, M.T. Leddy, K.D Gemmell and A.M Dollar. "Comparative Clinical Evaluation of the Yale Multigrasp Hand." *IEEE RAS Int. Conf. on Biomedical Robotics and Biomechatronics*, Singapore, 2016.
[25] J.G. Burgerhoff, E. Vasluian, P.U. Dijkstra, R.M. Bongers and C.K. Van Der Sluis. "The Southampton Hand Assessment Procedure revisited: A transparent linear scoring system, applied to data of experienced prosthetic users." *Journal of Hand Therapy*, Vol.30 pp.49-57, 2017.
[26] M. Deijs, R.M. Bongers, N.D.M. Ringeling-Van Leusen and C.K. Van Der Sluis. "Flexible and static wrist units in upper limb prosthesis users: functionality scores, user satisfaction and compensatory movemetns." *Journal of NeuroEngineering and Rehabilitation*, Vol.12, No. 26, 2016.
[27] M. Luchetti, A.G. Cutti, G. Verni, R. Sacchetti and N. Rossi. "Impact of Michelangelo prosthetic hand: Findings from a crossover longitudinal study." *Journal of Rehabilitation Research and Development*, Vol. 78, pp.307-323, 2014.
[28] O. Van Der Niet, R. M. Bongers and C.K. Van Der Sluis. "Functionality of i-Limb and i-Limb Pulse hands: Case report." *Journal of Rehabilitation Research and Development*, Vol. 50, 2013.
[29] J.T. Belter and A.M. Dollar. "Performance Characteristics of Anthropomorphic Prosthetic Hands." *IEEE Int. Conf. on Rehabilitation Robotics*, Switzerland, 2011.
[30] R. Vinet and Y. Lozac'h. "Design methodology for a multifunctional hand prosthesis," *Journal of Rehabilitation Research and Development,* Vol. 32, No. 4, pp. 316-324, 1995.
[31] N. Dechev, W.L. Cleghorn and S. Neuman. "Multiple finger, passive adaptive grasp prosthetic hand." *Mechanism and Machine Theory*, Vol. 36, pp. 1157-1173, 2001.